Aerosol and Air Quality Research, 12: 722–732, 2012
Copyright © Taiwan Association for Aerosol Research
ISSN: 1680-8584 print / 2071-1409 online
doi: 10.4209/aaqr.2012.02.0023

Assessment of Responsibility for Pollution from PM_{10} and Sulfur Dioxide and Application to an Industrial Area on the Northeastern Coast of Venezuela

Gladys Rincón[1,2*], Lázaro V. Cremades[2]

[1] *Departamento de Procesos y Sistemas, Universidad Simón Bolívar, Apdo. Postal 89000, Caracas 1080-A, Venezuela*
[2] *Departament de Projectes d'Enginyeria, Universitat Politècnica de Catalunya (UPC), ETSEIB, Av. Diagonal 647, Planta 10, 08028 Barcelona, Spain*

ABSTRACT

This study proposes a methodology to determine the origin of industrial emissions in order to attribute responsibility to the industries that pollute nearby towns. The methodology has been applied to the industrial area on the northeastern coast of Venezuela. This area is close to six densely populated towns. The study also gives the estimated PM_{10} and SO_2 levels in the towns adjacent to 11 industries, through modeling the dispersion of air pollutants from stationary sources. The model used has been the Lagrangian particle model LADISMO. The results are discussed by comparing the estimated values by the model with the limits proposed by the World Health Organization and United States Environmental Protection Agency.

Keywords: PM_{10}; Sulfur dioxide; Dispersion modeling; Assign responsibilities; Air quality.

INTRODUCTION

Assessing levels of PM_{10} (particulate matter with an aerodynamic diameter of up to 10 µm) and SO_2 (sulfur dioxide) in urban areas is crucial due to the harmful effects that these contaminants could cause on human health. This is even more evident if the urban centers coexist with high industrial activity, as in the northeastern coast of Venezuela at the north of Anzoátegui state. In this region (less than 500 km^2), there are six densely populated towns close to 11 heavy industries: one cement industry (IC), one petroleum refining industry (IRP), and nine facilities located in the Jose Industrial Complex (CIJ) - four oil upgrading industries (IM), four petrochemical industries (IP) and one gas fractionating industry (IFG).

Some air quality studies focused on particulate matter have been developed for the two main cities of Venezuela (Caracas and Maracaibo) (Ramírez *et al*., 1994; Fernández *et al*., 2001; García *et al*., 2002, Machado *et al*., 2007). But to date, there are no studies to assess air quality on the coast of the Anzoátegui state, even though the population has made complaints about the quality of air (MARNR, 2006).

It is known an inventory of emissions from the 11 heavy industries mentioned above, which accounted for 4790 t TSP/year and 8376 t SO_2/year. The emissions of TSP (Total Suspended Particles) were emitted from 92 sources (83 chimneys and 9 area sources), and the emissions of SO_2 from 81 chimneys (Cremades and Rincón, 2011).

The presence of both pollutants enhances the harmful effect of particulates on human health (Seinfeld and Pandis, 1998). The smallest particle sizes ($PM_{2.5}$ or PM_{10}) are not regulated in Venezuela. $PM_{2.5}$ means particulate matter with an aerodynamic diameter of up to 2.5 µm.

Identifying the relative contribution of the pollutant emission sources has been addressed from the study of chemical composition of emissions measured. These studies have allowed us to identify the type of emission source: mobile, fuel burning, cement industry, minerals industry, oil industry, dust, soil and marine aerosols (Donald *et al*., 1975; Kowalczyk *et al*., 1978, Kowalczyk and Gordon, 1982; Landen *et al*., 2000).

In this research, the type of emission source is identified, but the contribution of each pollution source of particulate matter and sulfur dioxide about air quality is unknown. Hence, this paper proposes a methodology to determine the origin of air pollution in towns coming from industrial emissions, in order to attribute responsibility, if any, to individual industries. This methodology has been applied to a real case in the industrial area on the northeastern coast of Venezuela (north cost of Anzoátegui state). It is based on modeling the dispersion of pollutants to make a diagnosis of air quality in the region by estimating the PM_{10} and SO_2 concentrations in nearby towns to the 11 industries.

MODEL FOR SIMULATING THE PARTICLE DISPERSION

* Corresponding author. Tel.: 58-212-9063331;
Fax: 58-212-9063304
E-mail address: grincon@usb.ve

The mathematical model used, called LADISMO (LAgrangian DISpersion MOdel) (Hernández, 1995), simulates the transport and dispersion of a pollutant from multiple emission point sources, non-steady state (episodic model) at meso-local level, taking into account the terrain and the 3-D wind field. LADISMO is divided into two submodels (Hernández *et al*., 1994, Hernández *et al*, 1997): one diagnostic model and one dispersion model. The first is responsible for creating a three-dimensional wind field using the variational method of zero divergence. Output from this model is sent to the dispersion model to calculate the pollutant dispersion, through a Lagrangian particle model. This model allows to know the source of emissions, and then can be attributed to each source its responsibility for the pollution.

The diagnostic submodel can simulate meteorological situations of special interest (anticyclonic situations, breezes, etc.) from actual measured meteorological data (upper and surface air data). Quality of simulation depends largely on the number of available meteo stations and their location. The more stations and the better distributed are within the study domain, the better the confidence of the interpolated wind field. This submodel takes into account the terrain, but does not consider the compressibility of the air.

LADISMO model simulates the dispersion of pollutants by considering that the plume consists of a large number of Lagrangian particles that individually represent a fraction of the mass of pollutant emitted. This model uses the wind field estimated by the diagnostic model and generates a set of Lagrangian particles trajectories. Then, pollutant concentrations are estimated for different immission volumes on the ground depending on these trajectories.

Each Lagrangian particle is "tagged" from the moment that is emitted by the source. Its displacement in each time step is independent of the other particles. Motion of particles is represented in accordance with pseudo-velocities equal to the sum of average values of the wind components and turbulent wind fluctuations. The mean wind components are obtained from the diagnostic meteorological model, while wind fluctuations are simulated from the Langevin equation using a random number generator. The model simulates the dispersion of one pollutant at once.

Some works related to Lagrangian particle models (de Haan, 1999; Stohl *et al*., 1998) refer that each Lagrangian particle might be represented by a sphere of uniform or variable density. In our case, we have assumed that each particle is like a sphere of variable density distributed according to a Gaussian probability density, with a radius equal to 3σ, σ being the standard deviation. This sphere can be equated for calculation purposes as a group of many sub-particles (≈ 10 000) with different mass densities. Each sub-particle has its own weight in terms of its distance from the center of the sphere following the Gaussian probability function. The sum of the weights of all the sub-particles is equal to one particle mass (Cremades and Rincón, 2012).

Pollutant concentrations are calculated into some immission volumes (cylinders of height H (3 m) and radius R (1.5 km) placed on the ground). The height of the cylinder is equal to the height of the sampling stations (3 m) and covers the equivalent of three grid cells in the horizontal and one cell in the vertical. This radio allows immission volumes cover virtually the entire populated area without overlapping. A different distribution of immission volumes would provide information on the immission concentration in other places other than those tested.

When the entire "sphere" of a Lagrangian particle is located within the immission volume, it provides one unit. If the whole sphere of a particle is out of the immission volume, its particle mass is not counted. When part of the sphere of a particle is within the immission volume, its contribution in mass is proportional to the particle sphere inside the cylinder, taking into account its variable density. Finally, the concentration in an inmission volume is calculated as the sum of the mass contributed by all particles divided by the volume occupied by its cylinder.

LADISMO has been validated successfully in three cases: 1) Castellón power plant located at the Spanish Mediterranean coast (Hernández *et al*., 1994) where emissions of SO_2 came from two 150 m height stacks, whose releases varied from 1,000 to 6,500 g/s, and 2) and 3) Guardo power plant located at the mountain of Palencia province, north central Spain (Hernández and Cremades, 1997). Case 2 refers to an elevated release of SF_6 gas tracer (185 m agl - above ground level) during neutral and synoptically dominated conditions with high winds (> 5 m/s), low temperatures and adiabatic stratification. Case 3 refers to a release of SF_6 gas tracer from a valley floor during drainage flow with light and apparently stable conditions.

METHODOLOGY

Six study cases have been analyzed to establish responsibilities on the PM_{10} and SO_2 pollution in the north eastern coast of Venezuela (Anzoátegui state). LADISMO model has been run for each study case and for each pollutant separately.

This investigation was conducted for the most conservative scenario from the standpoint of pollution. For that, it has been assumed that there was no pollution prior to starting the simulation time (zero background), which is equivalent to assuming that hours before a heavy rain had fallen (it would have happened or not). Potential PM_{10} and SO_2 emissions were limited to the eleven industries, without accounting for natural emissions of dust, emissions from mobile sources and emissions from other industries in the region. Deposition rate of pollutants was assumed equal to zero and no chemical reactions in the air.

Study domain topographic information was extracted from raster data models (SRTM, 2009). Emission data and geometric and operational characteristics of chimneys came from a 2006 emission inventory (Cremades and Rincón, 2011). It was assumed that pollutant rates remain constant throughout the year. Table 1 shows the 2006 emissions inventory for the eleven industries considered.

Immission volumes have been located in sites with the highest population density, taking care that there was no overlap between them. Immission volumes remained constant in all cases. Meteorological information came

Table 1. 2006 emissions inventory (Cremades and Rincón, 2011).

ID	Industries	TSP (t/year)	No. emission sources	SO_2 (t/year)	No. emission sources
IM1	Oil upgrading industry 1	309	9	357	14
IM2	Oil upgrading industry 2	139	7	685	10
IM3	Oil upgrading industry 3	64	8	364	9
IM4	Oil upgrading industry 4	54	13	5402	20
IP1	Petrochemical industry 1	114	3	17	3
IP2	Petrochemical industry 2	23	2	11	2
IP3	Petrochemical industry 3	245	2	13	3
IP4	Petrochemical industry 4	30	3	68	4
IF	Gas Fractionating industry	1 113	9	15	7
IRP	Petroleum Refining industry	1 434	10	1 348	3
IC	Cement industry	1 209	18	96	6
	IC sources area	29	5	-	-
	IM sources area	27	4	-	-
	Total emission and emission sources	4 790	92	8 376	81

from experimental data. Their resolution was one hour. After a series of preliminary tests, the simulation duration was set equal to 72 hours. PM_{10}-24h concentration has been estimated from TSP-24h value: to this, a PM_{10}-24h/TSP-24h ratio equal to 0.402 ± 0.122 has been used (Rincón *et al*., 2010).

A qualitative analysis has been carried out to estimate which emission sources impact a greater number of times on each immission volume. Emission sources have been grouped first by type of emission source (area sources and point sources) and, second, by type of industry: cement, petroleum refining, upgrading, petrochemical, gas fractionating.

"Actual impact" has been defined as the number of Lagrangian particles reaching the immission volumes and "likely impact" as the amount of actual impacts from each industry on the total of actual impacts expressed as a percentage. To set a ordered list of the most polluting industries, the "likely impact" from each industry is calculated for the two pollutants (PM_{10} and SO_2) separately. The most polluting industry is that with the most likely impact. The industries are sorted in descending likely impact.

To estimate the distribution of each pollutant from each industry on the municipalities, the "actual impact" in each municipality is calculated for each industry and pollutant separately, and divided by the total of "actual impacts" for all municipalities. Qualitative analysis alone is not enough to attribute responsibility to the emission sources, since this analysis does not take into account the importance of impact.

A quantitative analysis has been also carried out to know the pollutant concentration in each immission volume. In total, 52 immission volumes were used for estimating the pollutant concentrations in towns. Concentration in the immission volumes are estimated by assuming a radius of influence (radius of the spherical Lagrangian particle) = 75 m. This value has been established based on previous studies (Cremades *et al*, 2000) and specific tests for this case (Rincón, 2010).

The pollutant concentration has been estimated as the mass of pollutant in each immission volume divided by the volume occupied by this immission volume. Daily pollutant concentration has been calculated by averaging the 24 hourly pollutant concentrations.

REAL CASE: INDUSTRIAL AREA ON THE NORTHEASTERN COAST OF VENEZUELA

Study Domain

The domain of study is located in the northern state of Anzoátegui, 80 × 90 km^2 on surface, between the southwest corner in Universal Transverse Mercator (UTM) coordinates: X = 255000 m, Y = 1070400 m, and the northeast corner: X = 345000 m, Y = 1150400 m, zone 20, datum WGS 84 (Fig. 1). The highest altitude is 1042 m agl and the lowest altitude is 0 m agl (the ocean). This domain fully covers the following municipalities: Bolivar (whose capital is Barcelona), Sotillo (Puerto La Cruz), Guanta (Guanta), Urbaneja (Lechería), Píritu (Píritu) and Peñalver (Puerto Píritu). Additionally, the domain of study covers partly the following municipalities: Libertad, Bruzual y Cajigal (Fig. 1). The domain has a horizontal resolution of 1 km and 11 vertical layers (0, 6, 12, 50, 100, 200, 400, 800, 1,500, 5,000, 10,000 meters agl).

Orography of the region contains beaches, plains and mountains, with a number of coastal landforms caused by the collision of the eastern mountain range to the sea. This mountain range has abundant vegetation. The urban and industrial areas are concentrated on the coast. Land uses have been grouped into eight categories: Urban, Suburban, Industrial, Pasture, Crops, Bushes, Wood, Water.

Meteorology

Venezuela is located in a intertropical area of equatorial low pressures blowing northeastern trade winds in its coasts. As a result of the general circulation of the atmosphere, there are two periods commonly called "summer" (dry season) between December and April, and "winter" (rainy season) between May and November. Some temperature inversions (known as "trade winds inversions") are usually produced at altitudes close to 3000 m agl (Goldbrunner,

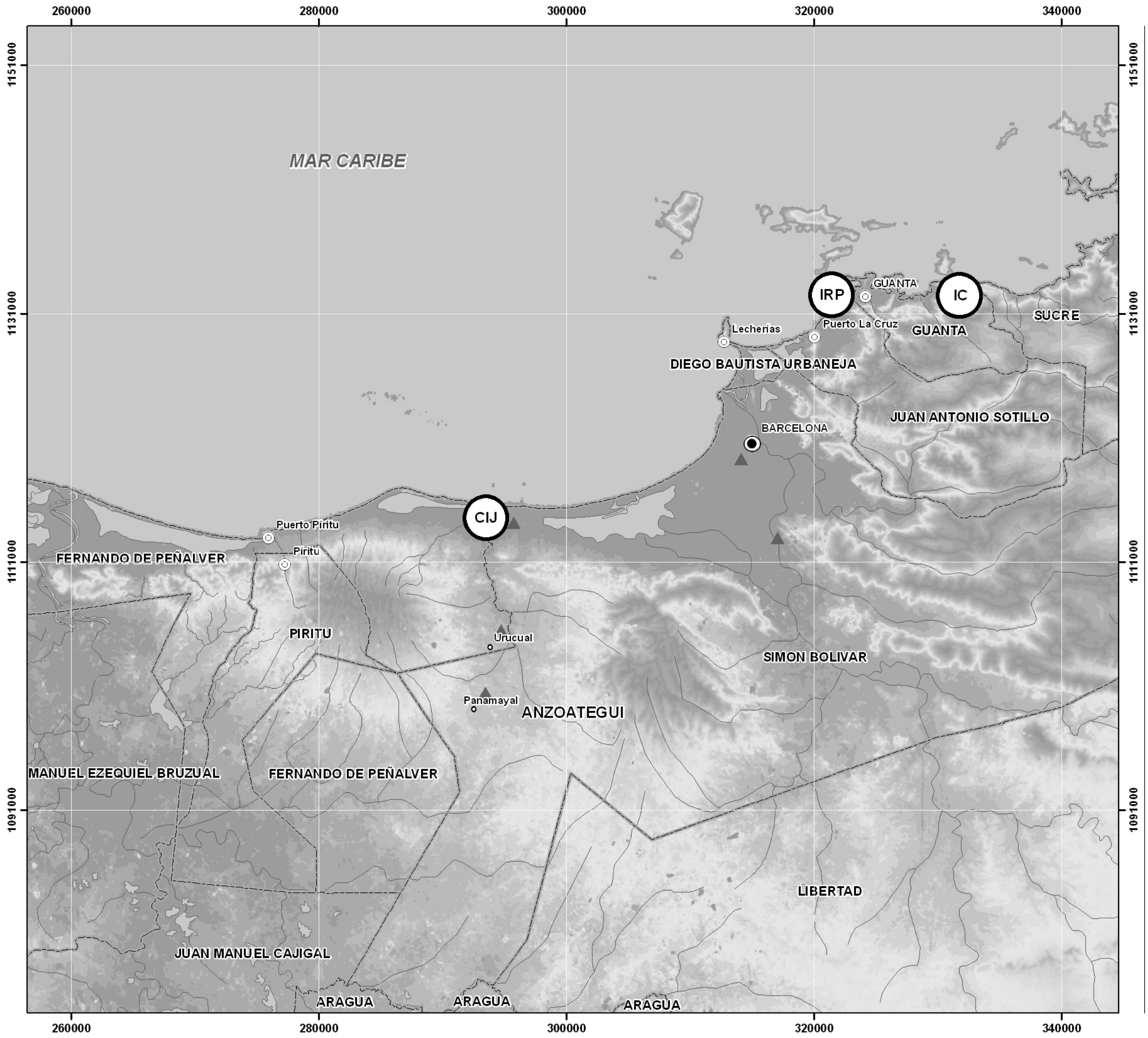

Fig. 1. Study domain. Hypsometric map in m agl (northeastern coast of Venezuelan). Boundaries of municipalities are drawn as gray lines; surface meteo stations and upper air point as dark gray triangles; industries as white circles. CIJ, complex industrial; IRP, petroleum refining industry; IC, cement industry.

1984). Temperature shows little change with season, but can have some variations depending on the proximity to ocean and/or altitude.

According to a climatological study for the period 1951–1970 (Goldbrunner, 1984), the study area is semi-wet, having annual rainfall between 600-900 mm. The absolute maximum and minimum temperatures in this region are between 14.0 and 39.7°C. There is a strong presence of northerly winds (N, NNE, NNW) combined with less frequent winds from the south (S, SSE, SE, ESE) and with some westerly winds (W). These directions may result from the influence of the northeast trade winds combined with some local effect by the landforms of coasts (Alvarez, 1983). Speed of prevailing wind ranges between 2.5 and 6.5 m/s, with a higher presence of light winds overnight.

For this study, surface hourly meteo data at four stations (Airport, Cryogenic, Urucual and Panamayal, see Fig. 1) were available for the year 2006 and for the following variables: temperature, pressure, relative humidity, solar radiation, wind speed and direction. However, for not documented reasons, the stations had not all the expected records per year. Fig. 2 shows the windroses of Airport station for 2000–2007, Cryogenic station for 2004–2006, Urucual station for 2006 year and Panamayal station for 2006. It shows the prevalence of northeast winds at Cryogenic and Panamayal stations, winds from North and South at Airport station (possibly by the effect of land-sea breeze), and north-northwest winds in the Urucual station, possibly due to the effect of a mountain canyon at the entrance to Píritu.

Experimental upper air data were not available for the study domain. But, because that information is essential to study the dispersion of pollutants in the air, these data were obtained from the official website of the National Oceanic and Atmospheric Administration *(*NOAA) sounding section - GDAS (Global Data Assimilation Systems) (ARL, 2009), for the location X: 317092 m, Y = 1113000 m in UTM coordinates, at times 1:30, 7:30, 13:30, 19:30 LST (local standard time) and for layers comprised between 240 and 10,000 m agl.

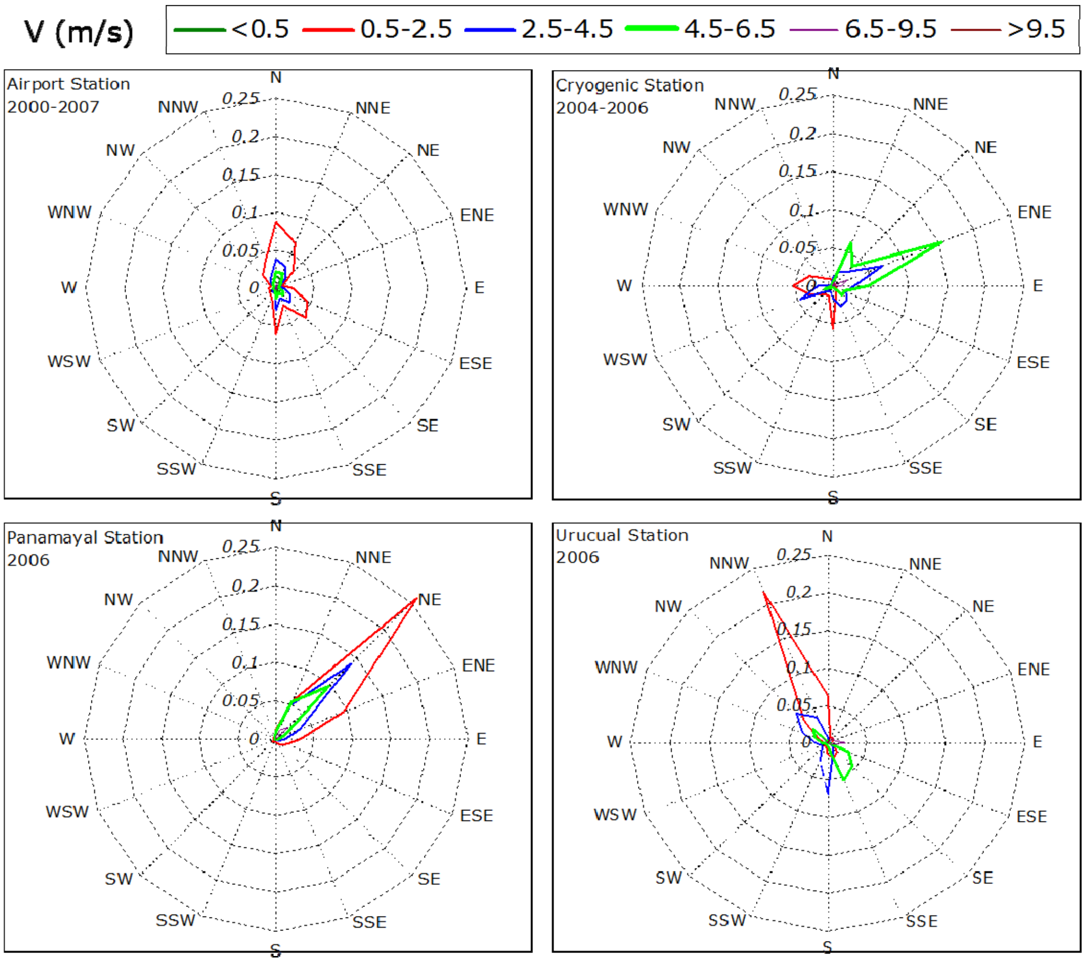

Fig. 2. Windroses from wind data recorded at the meteorological stations: Airport, Cryogenic, Urucual and Panamayal. v: wind speed.

By analyzing these vertical sounding data for 2006, the vertical temperature gradient is usually between –1.5 and –0.5 °C/100 m, showing a neutral stability condition. But it has also often found for the first layer between 240 and 305 m agl that the vertical temperature gradient at night is between 0.015 and 0.030 °C/100 m, showing a slightly stable behavior. The slightly stable condition tends to run over 3,000 m agl (between layers 9th and 10th), which could correspond to the phenomenon known as "trade winds inversions" that occurs over most of Venezuela (Goldbrunner, 1984). Fig. 3 shows as an example the vertical temperature gradient on 13 FebruPary, 2006. At 01:30 LST the vertical profile of air temperature at the first layer remains constant with the altitude. The other profiles, after sunrise, show a sharp decrease in temperature in the first layers.

DESIGN OF CASES: INDUSTRIAL AREA ON THE NORTHEASTERN COAST OF VENEZUELA

Surface wind direction and vertical temperature gradient show the highest variability with seasons. Surface winds at the Cryogenic station showed three patterns: 1) between February and May, winds from NE, 2) between May and September, winds from S and SE, and 3) between September and December, winds from W and from NE. Winds at the Airport station showed two patterns: 1) from February to September, winds from NE combined with winds from SE, and 2) from September to February, winds from the south (S, SSE, SE). The stations in the continent (Urucual and Panamayal) showed little variability in wind direction throughout the year: Panamayal showed NE and NNE winds, while Urucual had prevailing winds from West and a very low frequency of winds from South (< 1%).

It was expected to have at least 121 periods of 72 hours for the year 2006, but complete meteo information for all variables in the four stations was available only in 28 periods. Six periods were selected from these 28 periods with full information. They are representative of the three patterns in surface wind direction at Cryogenic station and of the two patterns in the Airport station. It was verified that these periods were also representative of upper winds. The dates selected for the six cases are showed in the Table 2. Cases 1, 4, 5 and 6 show stable thermal stratification between 250–300 m agl.

Distribution of immission volumes in the municipalities has been: 2 in Lecherías, 4 in Puerto La Cruz, 6 in Guanta, 24 in Barcelona, 7 in Puerto Piritu, 7 in Píritu, 1 in Urucual, and 1 in Panamayal. In order to cover the large area

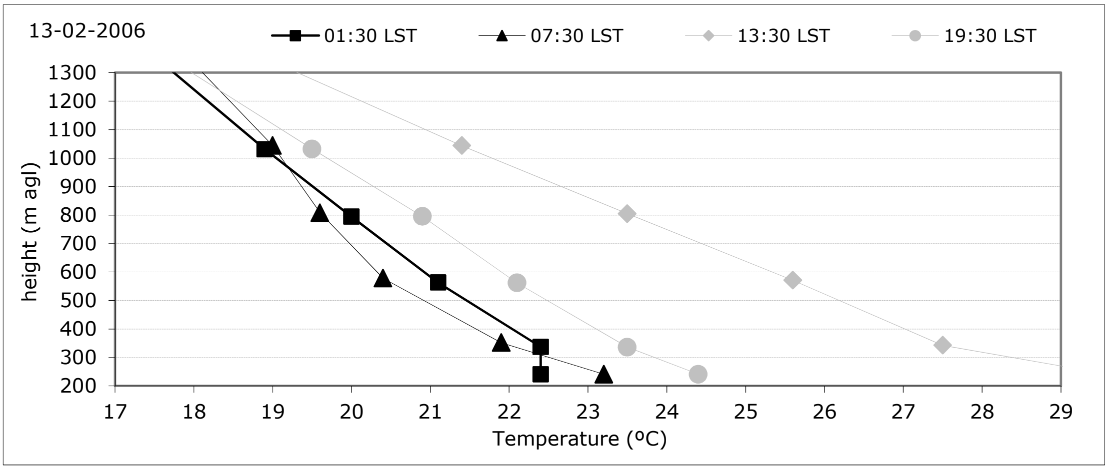

Fig. 3. Vertical temperature gradient on 13 February, 2006, for the location X: 317,092 m, Y = 1,11,000 m, in UTM coordinates. agl: above ground level.

Table 2. Dates selected for the six study cases.

Case	Date
Case 1	13 to 15 February, 2006
Case 2	20 to 22 March, 2006
Case 3	8 to 10 June, 2006
Case 4	10 to 12 July, 2006
Case 5	2 to 4 October, 2006
Case 6	26 to 28 October, 2006

occupied by the population centers of Barcelona, has been necessary to use a larger number of immission volumes. In 2006, the region had two sampling sites where TSP was collected for 24 hours every six days: Barcelona and Puerto La Cruz stations. There were no SO_2 sampling stations.

ACCURACY OF THE LADISMO MODEL

The results of the application of the diagnosis meteorological submodel of LADISMO in generating three-dimensional wind fields in the study area have been evaluated by comparing the values of speed and wind direction observed and calculated in the four meteorogical stations. As an example, Table 3 shows some calculated and observed values at meteorological stations Criogénico and Panamayal on 13 February, 2006.

The following statistics have been applied to the series of 72 pairs of data (observed and calculated) at each meteo station for the six cases: RMSE (root mean square error), MAE (mean absolute error), FB (fractional bias), NMSE (normalised mean square error). As an example of the evaluation of the diagnostic model, Table 4 shows the results of these statistical indices in Criogénico and Panamayal stations and for the six cases.

Table 4 shows that the diagnostic submodel can reproduce a wind field with a good degree of adjustment to the observed data. Each value represents a estimation of the average advective wind conditions in the volume of the grid cell. This value is compared with point measurements which are representative of a horizontal scale with a length less than that of the grid cell. The statistics indicate that the overall fit of the wind field is reasonable and is within the working standards of the type of model used.

To evaluate the accuracy of the LADISMO dispersion submodel there is available a small number of data pairs of pollutant concentration (measured and calculated) in the towns, because the concentrations of TSP-24 h are only measured each six days at two sampling sites, and the dates of collection does not necessarily coincide with the date of the third day of simulation in the six cases.

Table 3. Observed and calculated values of wind speed and direction in Cryogenic and Panamayal stations for the six study cases.

Station	LST	Wind speed (m/s)		Wind direction (°)	
		Observed	Calculated	Observed	Calculated
Criogénico	00:00	5.40	5.46	81.90	81.60
	06:00	2.90	2.93	85.10	84.60
	12:00	4.45	4.55	61.80	62.60
	18:00	6.25	6.37	69.80	70.60
Panamayal	00:00	0.54	0.54	181.50	181.60
	06:00	3.68	3.69	23.10	23.60
	12:00	6.45	6.49	35.20	35.60
	18:00	4.26	4.32	28.20	28.60

LST: Local Standard Time.

Table 4. Evaluation results of the diagnostic meteorological model LADISMO.

	Case	Wind speed				Wind direction			
		RMSE (m/s)	MAE (m/s)	FB	NMSE	RMSE (°)	MAE (°)	FB	NMSE
Criogénico station	1	0.0857	0.0596	–1.23E-04	5.04E-06	0.7525	1.0625	9.94E-07	3.97E-07
	2	0.0727	0.0696	–8.33E-04	1.50E-05	0.7945	0.6957	–5.3E-06	1.52E-06
	3	0.1145	0.0890	–1.39E-03	5.33E-05	0.6786	0.5136	1.21E-06	7.60E-07
	4	0.0856	0.0662	–3.28E-04	1.05E-05	0.9106	1.2417	3.79E-06	4.20E-07
	5	0.0857	0.0596	–1.18E-04	5.04E-06	0.7525	1.0625	9.94E-07	3.97E-07
	6	0.0827	0.0736	–1.00E-03	2.91E-05	0.6391	0.4903	8.12E-06	2.60E-07
Panamayal station	1	0.0754	0.0558	–3.31E-04	3.72E-06	0.7144	0.5826	–1.4E-06	1.02E-06
	2	0.0645	0.0558	–1.38E-04	1.85E-06	1.1816	0.8913	4.36E-06	4.88E-06
	3	0.0859	0.0677	–7.63E-04	1.56E-05	1.8532	1.3619	–8.6E-06	6.80E-05
	4	0.0879	0.0764	–3.81E-04	1.69E-05	0.9765	1.3579	5.00E-06	4.45E-06
	5	0.0786	0.0529	–5.60E-04	8.13E-06	0.8610	0.6591	1.06E-05	1.40E-05
	6	0.0776	0.0526	–6.51E-04	1.12E-05	0.8299	0.7391	8.86E-06	2.75E-06

RMSE: root mean square error; MAE: mean absolute error; FB: fractional bias; NMSE: normalised mean square error.

Although data are not enough to establish quantitatively the accuracy of the dispersion model, Table 5 shows the TSP-24 h concentration values, measured and calculated, for the third day of simulation of the six cases modeled at two sampling stations: Barcelona y Puerto La Cruz. Blank cells correspond to days in which TSP samples were not collected. It is emphasized that the TSP sampling stations are located in high vehicular traffic areas in Barcelona and Puerto La Cruz cities. Table 5 shows that the measured and calculated values are on the same order of magnitude, but the measured values are higher, maybe due to the location of sampling stations.

AIR QUALITY: PM_{10} AND SO_2

As an example, Fig. 4 shows the path of Lagrangian particles for PM_{10} emissions, on XY and XZ planes for the simulation hour 72 and for cases 4 and 5. The path of the pollutant shown in the XY plane corresponds with that in XZ (although for clarity purposes, only 60% of Lagrangian particles are shown). Dispersion for both pollutants (PM_{10} and SO_2) has been similar because LADISMO simulates the dispersion of fine particulate matter like a gas and assumes that sulfur dioxide does not undergo secondary chemical reactions.

For case 4, the path of pollutants is a result of light winds from south and winds from east move the pollutants towards the sea. In case 5, the trajectory is a result of a combination of directions: W, NNE, NE, ENE, SSE, ESE, causing a tendency to concentrate the pollutants on population centers. For case 4, XZ plane in Fig. 4 shows the highest pollutant concentration at relatively low altitudes, possibly due to a stable thermal stratification.

From the results of the six cases a hierarchy of emission sources has been established based on their contribution to pollution on population centers. Area sources are the ones with the highest contribution of PM_{10} pollution on towns (79%), and in turn, 99% of these immissions come from the cement industry (IC): baggers, conveyors, bulk cement dispatch. TSP emissions from area sources in the cement industry were 29 tons/year (0.60% of total) (Cremades and Rincón, 2011). Since these emissions are emitted at low temperature and low emission height and the cement industry is located near urban areas, they can easily reach

Table 5. Observed and calculated values of concentration of TSP-24 hours for the third day of simulation in the six study cases.

Station	Sampling date	TSP-24 h (μg/m^3)		
		Observed (o)	Calculated (c)	Difference (o-c)
Barcelona	15-Feb-06		267	
	22-Mar-06		75	
	10-Jun-06		15	
	12-Jul-06	73	50	23
	04-Oct-06	53	33	20
	28-Oct-06	43	31	12
Puerto La Cruz	15-Feb-06		145	
	22-Mar-06		38	
	10-Jun-06		78	
	12-Jul-06	134	103	31
	04-Oct-06	93	72	21
	28-Oct-06	113	116	–3

Empty fields in TSP observed are due to lack of measurements in that date.

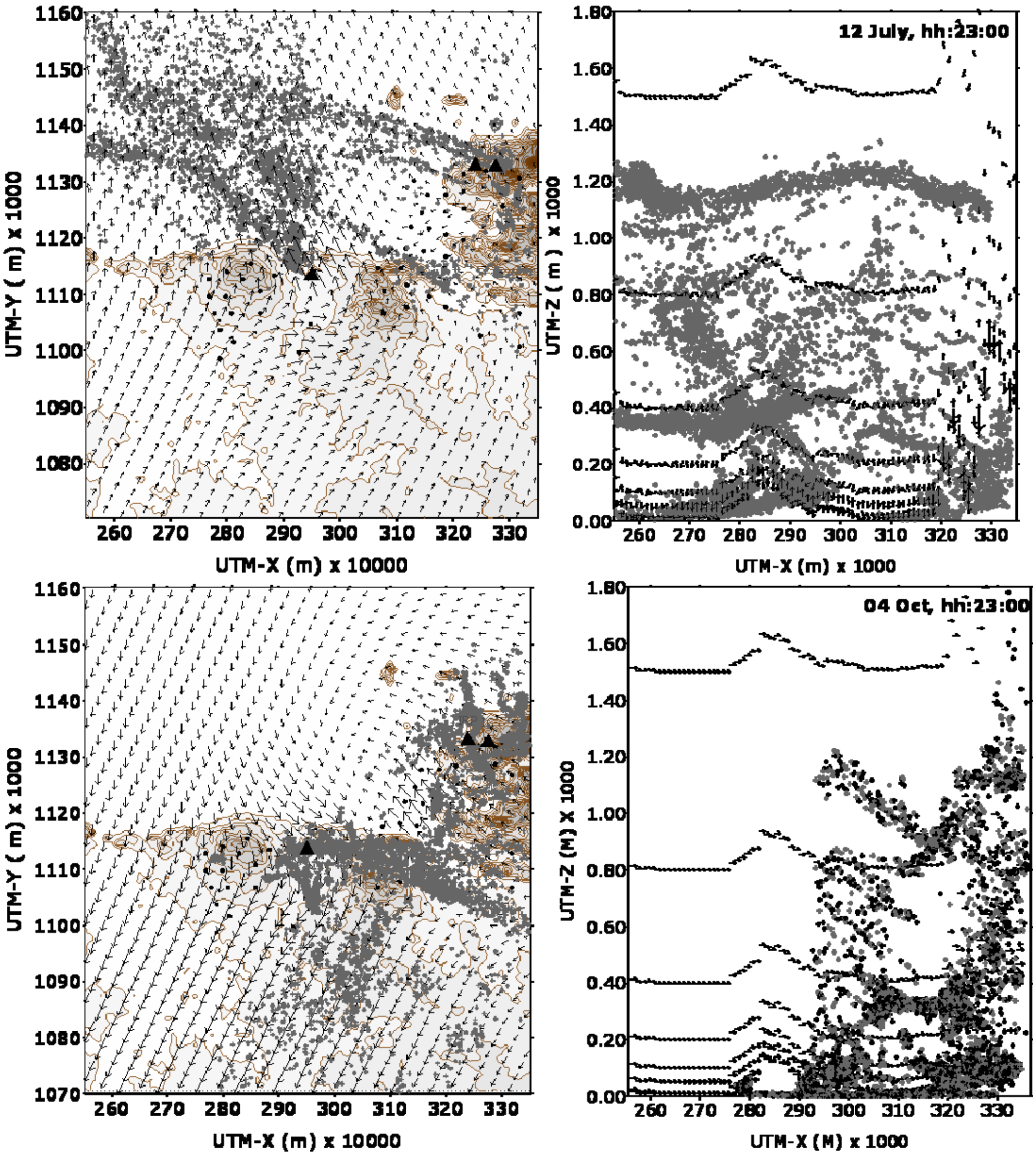

Fig. 4. Graphic representation of XY and XZ sections showing the modeling results of PM_{10} dispersion for cases 4 and 5 (07/12/2006 and 10/04/2006), marked with gray dots. Surface wind is marked with arrows representing the wind direction. For clarity purposes, only 60% of Lagrangian particles are shown.

the surrounding towns. There were no SO_2 emissions from area sources.

Fig. 5 shows the ordered list of industries that pollute from point sources (furnaces, incinerators, boilers, generators, burners, mills). It also shows the share of responsibility for each type of industry in pollution. The oil upgrading industries (IM) are mainly responsible for pollution over urban areas: 51.5% of PM_{10} and 89.2% of SO_2. PM_{10} emissions from point sources in the cement industry also have an important contribution to pollution (27.4%).

Proportion of pollution impact in towns per industry (point sources) is shown in Fig. 6. This figure shows that the most polluted city by point sources is Barcelona (Bcn) regardless of the pollutant. This may be due to the large area occupied by the town or to being surrounded by all industries. Guanta (Gua) receives 90% of the emissions from area sources of the cement industry.

World Health Organization (WHO, 2005) warns about the risk of increased mortality of about 0.5% for each increase of 10 $\mu g/m^3$ in the daily concentration of PM_{10}. Fig. 7 shows the PM_{10}-24h concentration field in the region for the maximum concentration values in the six cases, indicating also the location of industries and immission volumes. The light gray areas indicate the areas with safe concentration levels according to WHO criteria. The medium gray areas meet the U.S. Environmental Protection Agency standard (US EPA, 2006) and the dark gray areas have pollution levels above the US EPA standard. PM_{10} is mainly concentrated in the vicinity of the cement industry (industry with the highest responsibility for PM_{10} immission) reaching unsafe values for human health. There is no TSP or PM_{10} sampling station near the cement industry.

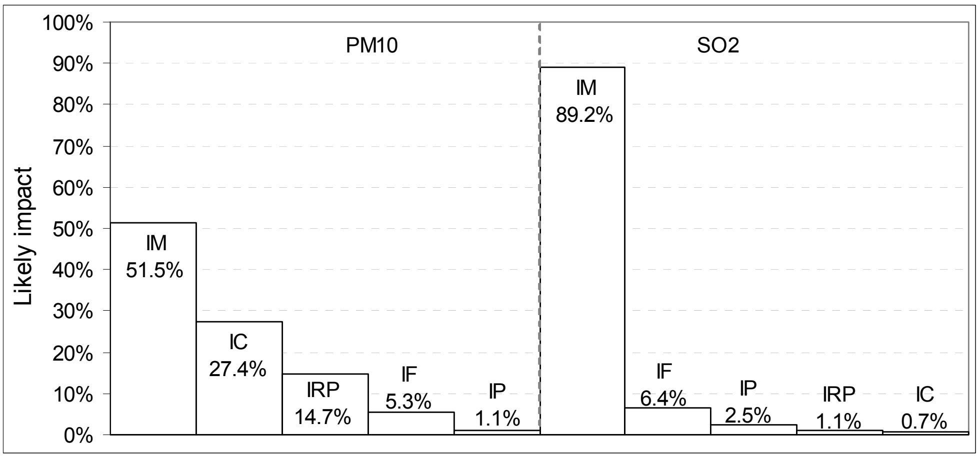

Fig. 5. Ordered list of industries ranked according to their likely polluting impact of PM_{10} and SO_2, separately. IM, oil upgrading industries; IP, petrochemical industries; IF, gas fractionating industry; IRP, petroleum refining industry; IC, cement industry.

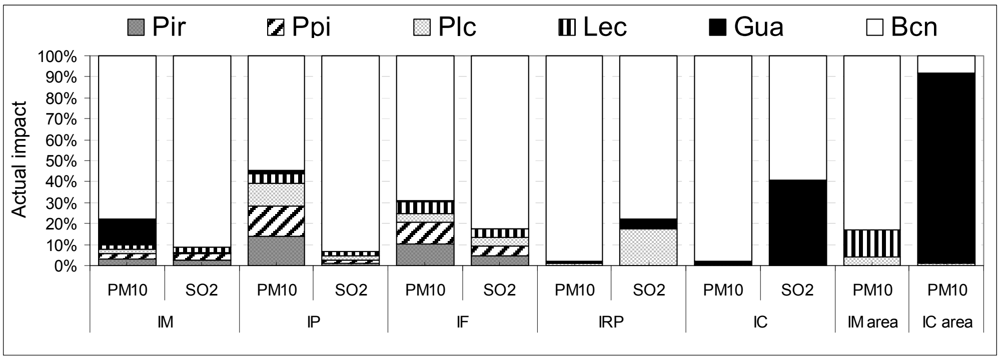

Fig. 6. Distribution of impacts of PM_{10} and SO_2 from point sources. Bar, Barcelona city; Plc, Puerto La Cruz city; Gua, Guanta city; Pir, Píritu city; Ppi, Puerto Píritu city. IM, oil upgrading industries; IP, petrochemical industries; IF, gas fractionating industry; IRP, petroleum refining industry; IC, cement industry; IM area, area sources oil upgrading industries; IC area, area sources cement industry.

WHO, under a precautionary approach, due to the uncertainty about health effects of SO_2, proposed a very strict limit value for SO_2-24 h (< 20 μg/m^3) against the standard in US EPA (< 365 μg/m^3). For SO_2-24h, Fig. 8 is equivalent to Fig. 7. It shows that virtually all urban areas are polluted by SO_2, reaching high risk levels in the central zone (Panamayal and Urucual). These results are consistent with claims made by these communities for smelling strong odors often and suffering from respiratory diseases (MARNR, 2006).

It is important to remember that these PM_{10} and SO_2 levels only include primary anthropogenic emissions from the 11 industries inventoried. Therefore, in any case, the actual levels of PM_{10} and SO_2 are likely to exceed these estimations.

CONCLUSIONS

The proposed methodology has been useful to objectively assign responsibilities to industries on the pollution that could affect certain pre-defined control volumes. The methodology allowed us to estimate which industries have greater responsibility for the pollution of particulate matter in the study area: cement industries (CI) and oil upgrading industries (IM). Similarly, IM are likely responsible for the SO_2 pollution.

Under a conservative scenario from the point of view of PM_{10} and SO_2 pollution, it could be said that people from Guanta and Barcelona have lived some risk episodes by particulate matter. On the other hand, people from Barcelona, Urucual and Panamayal could have been exposed to some episodes of SO_2 pollution, which sometimes could have reached much higher values than the threshold ones regulated by EPA (Environmental Protection Agency).

The LADISMO model has been able to simulate the dispersion of pollutants from 92 PM_{10} emission sources and 81 for SO_2 (separately) in the same study domain.

ACKNOWLEDGEMENTS

This research was sponsored by the Research Deanship of the Universidad Simón Bolívar through the project DI-CAI-001-07, the Venezuela´s Science, Technology and Innovation National Fund (FONACIT) through the Project

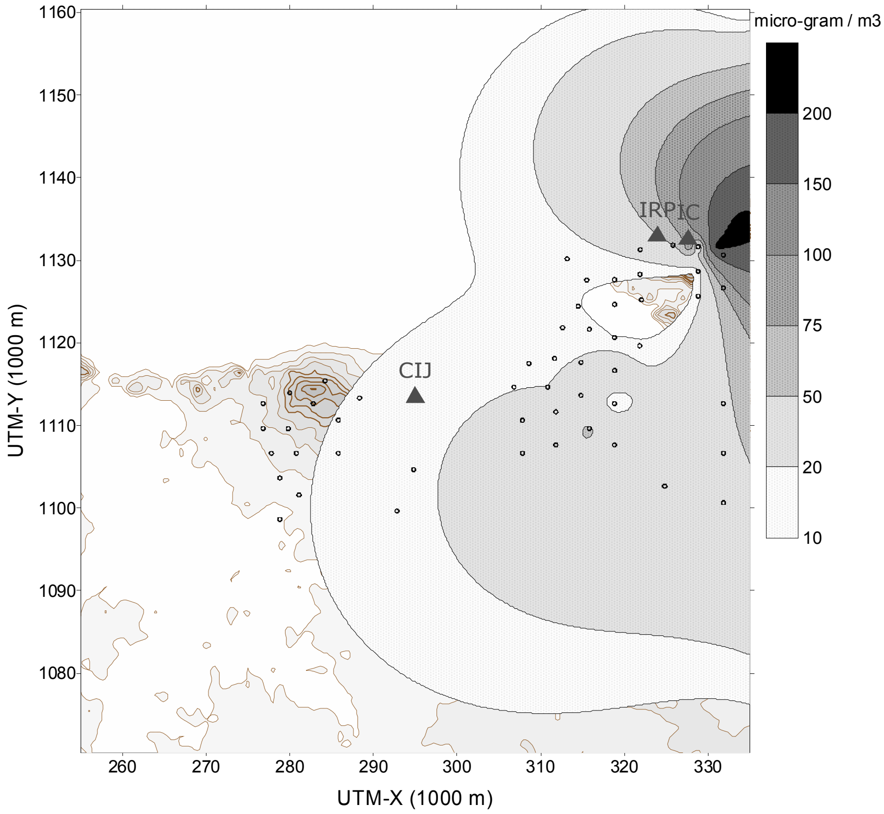

Fig. 7. Distribution of PM_{10} concentration on the XY plane of the study domain. Triangles represent the location of industries; spots represent the immission volumes. CIJ, complex industrial; IRP, petroleum refining industry; IC, cement industry.

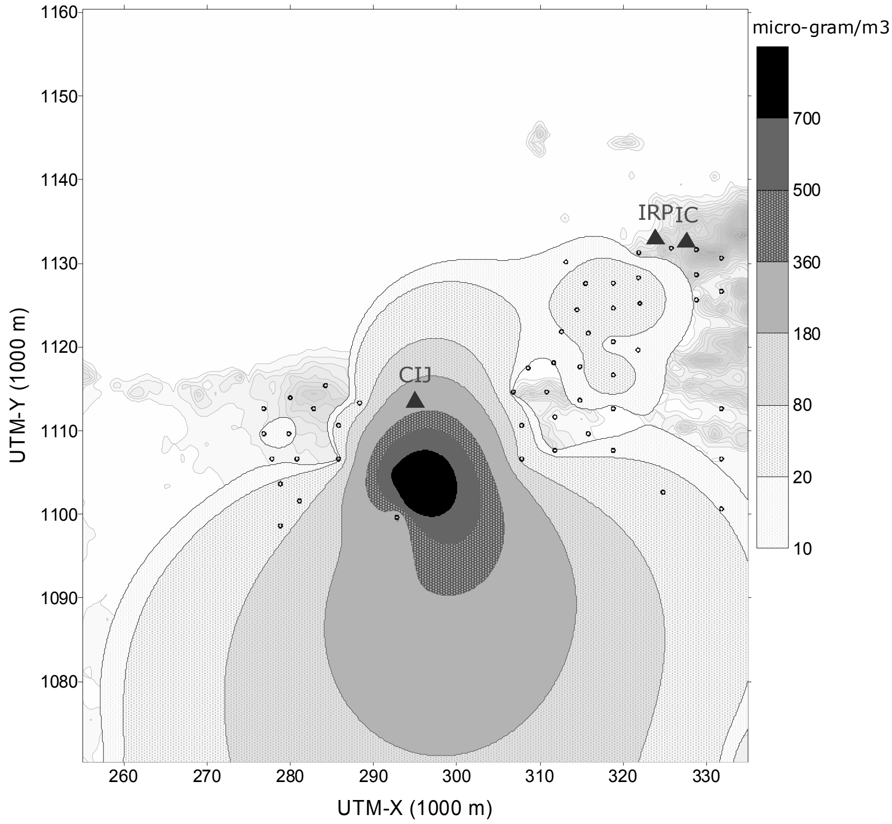

Fig. 8. Distribution of SO_2 concentration on the XY plane of the study domain. Triangles represent the location of industries; spots represent the immission volumes. CIJ, complex industrial; IRP, petroleum refining industry; IC, cement industry.

N°. 2005000432 and the Alfa/LignoCarb Program. Alfa 0412FIL. The authors wish to thank the staff of the Venezuelan Environmental Ministry (MARNR) who kindly provided the information.

REFERENCES

Álvarez, B.F. (1983). Atlas Climatológico de Venezuela. (Eds.), Universidad Central de Venezuela, Caracas, p. 132 [in Spanish].

ARL (2009). Air Recourse Laboratory of National Oceanic and Atmospheric Administration (NOAA), Archived Meteorology (on-line), URL: http://ready.arl.noaa.gov/READYamet.php (accessed on April 2010).

Cremades, L.V., García, D. and Roca, X. (2000). Estudio de Olores Industriales en áreas Urbanas. *Ing. Quim.* 32: 231–238. [in Spanish].

Cremades, L.V. and Rincón, G. (2011). Valoración Cualitativa de la Calidad de un Inventario de Emisiones Industriales en la Costa Nororiental de Venezuela. *Interciencia* 36:128–134. [in Spanish].

Cremades, L.V. and Rincón, G. (2012). Impact of Height and Location of Stacks in a Lagrangian Particle Model: Industrial Complex in Venezuela, Case Stud. *Revista de la Universidad del Zulia*. [pending approval].

de Haan, P. (1999). On the Use of Density Kernels for Concentration Estimations within Particle and Puff Dispersion Models. *Atmos. Environ*. 33: 2007–2021.

Donald, G.(1975). Relative Contributions of Different Sources of Urban Aerosols: Application. *Atmos Environ*. 9: 11–18.

Fernández, R. and Galarraga, F. (2001). Lead Concentration and Composition of Organic Compounds in Settled Particles in Road Tunnels from the Caracas Valley-Venezuela. *Environ. Geochem. Health*. 23: 17–25.

García, N., Machado, A., García, C., Socorro, E., Hernandez, H. and Granado, N. (2002). Concentraciones Atmosféricas de PTS y su Contenido de Metales en una Zona Adyacente a una Planta de Cemento. *Interciencia* 27: 476–481 [in Spanish].

Goldbrunner, A.W. (1984). Atlas Climatológico 1951-70. (Eds.), Ministerio de la Defensa, Fuerza Aérea, Comando Logístico, Servicio de Meteorología. República de Venezuela, p. 68 [in Spanish].

Hernández, J. (1995). Modelización de la Dispersión de Contaminantes Atmosféricos Según un Esquema Lagrangiano de Partículas, Ph.D. Thesis, Universitat Politècnica de Catalunya. Barcelona, Spain. 370 pp. [in Spanish].

Hernández, J.F., Cremades, L. and Baldasano, J.M. (1994). Dispersion Modeling of a Tall Stack Plume in the Spanish Mediterranean Coast by a Particle Model. *Atmos. Environ*. 29: 1331–1341.

Hernández, J.F. and Cremades, L. (1997). Simulation of Tracer Dispersion from Elevated and Surface Releases in Complex Terrain. *Atmos. Environ.* 31: 2337–2348.

Kowalczyk, G., Choquette, C. and Gordon, G. (1978). Chemical Element Balances and Identification of Air Pollution Sources in Washington, D.C. *Atmos. Environ.* 12: 1143–1153.

Kowalczyk, G., Gordon, G. and Rheingrover, S. (1982). Identification of Atmospheric Particulate Sources in Washington, D.C. Using Chemical Element Balances. *Environ. Sci. Technol.* 16: 79–90

Laden, F., Neas, L.M., Dockery, D.W. and Schwartz, J. (2000). Association of Fine Particulate Matter from Different Sources with Daily Mortality in Six U.S. Cities. *Environ. Health Perspect.* 108: 941–947.

Machado, A., Velázquez, H., García, N., García, C., Acosta, L., Córdoba, A. and Linares, M. (2007). Metales en PM_{10} y su Dispersión en una Zona de Alto Tráfico Vehicular. *Interciencia* 32: 312–317 [in Spanish].

MARNR (2006). Análisis de los Datos 2004 – 2006 de Calidad del Aire en las Comunidades Aledañas al Complejo Petrolero y Petroquímico Gral, José Antonio Anzoátegui. Technical Report, Ministerio del Ambiente y de los Recursos Naturales Renovables, Anzoátegui, 30 pp. [in Spanish].

Ramirez, A., Fernandez, A. and Fraile, R. (1994). Lead, Cooper and Zinc in Atmospheric and Fluvial Particulates from the Caracas Valley, Venezuela. *Environ. Geochem. Health* 16: 129–133.

Rincón, G. (2010). Análisis Integrado de la Calidad del Aire en la Costa Nororiental de Venezuela, Ph.D. Thesis, Universitat Politècnica de Catalunya, Barcelona, Spain. 217 pp. [in Spanish].

Rincón, G., Cremades, L.V. and Font, J. (2010). Estimation of PM_{10}/TSP Ratio: Air Quality Puerto La Cruz City, Venezuela, Book of Abstracts of the 21th Annual Conference of the International Environmetrics Society, a Section of the ISI, Guenni, L. and Llata, I. (Eds.), Venezuelas, p. 47.

Seinfeld, J. and Pandis, S. (1998). *Atmospheric Chemistry and Physics: From Air Pollution to Climate Change*. John Wiley & Sons, New York.

SRTM (2009). Shuttle Radar Topography Mission [online]. URL: http://srtm.usgs.gov/ (accessed on October 2009).

Stohl, A., Hittenberger, M. and Wotawa, G. (1998). Validation of the Lagrangian Particle Dispersion Model FLEXPART Against Large Scale Tracer Experiment Data. *Atmos. Environ.* 32: 4245–4264.

US EPA (2006). Us Environmental Protection Agency, National Ambient Air Quality Standards (NAAQS), (on-line), URL: http://www.epa.gov/air/criteria.html (accessed on April 2010).

WHO (2005). WHO/SDE/ PHE/OEH.06.02, WHO Air Quality Guidelines for Particulate Matter, Ozone, Nitrogen, Nitrogen Dioxide and Sulfur Dioxide - Global Update 2005 - Summary of Risk Assessment, Switzerland, 20 pp.

Received for review, February 1, 2012
Accepted, July 10, 2012